Supporting Information

Controlled pyrolysis of MIL-88A to Fe_2O_3@C nanocomposites with varied morphologies and phases for advanced lithium storage

Yang Wang, [a, b] *Xingmei Guo,* [a] *Zhenkang Wang,* [a] *Minfeng Lü,* [a] *Bin Wu,* [a] *Yue Wang,* [a] *Chao Yan,* [c] *Aihua Yuan,* [a, b] *and Hongxun Yang* [a, b, d,*]

[a]*School of Environmental & Chemical Engineering, Jiangsu University of Science and Technology, Zhenjiang 212003, Jiangsu, China,* [b]*Marine Equipment and Technology Institute, Jiangsu University of Science and Technology, Zhenjiang 212003, Jiangsu, China,* [c]*School of Material Science and Engineering, Jiangsu University of Science and Technology, Zhenjiang 212003, China,* [d]*Jiangsu Tenpower Lithium Co. Ltd., Zhangjiagang 215618, Jiangsu, China.*

*Corresponding author: E-mail address: yhongxun@126.com (Hongxun Yang);

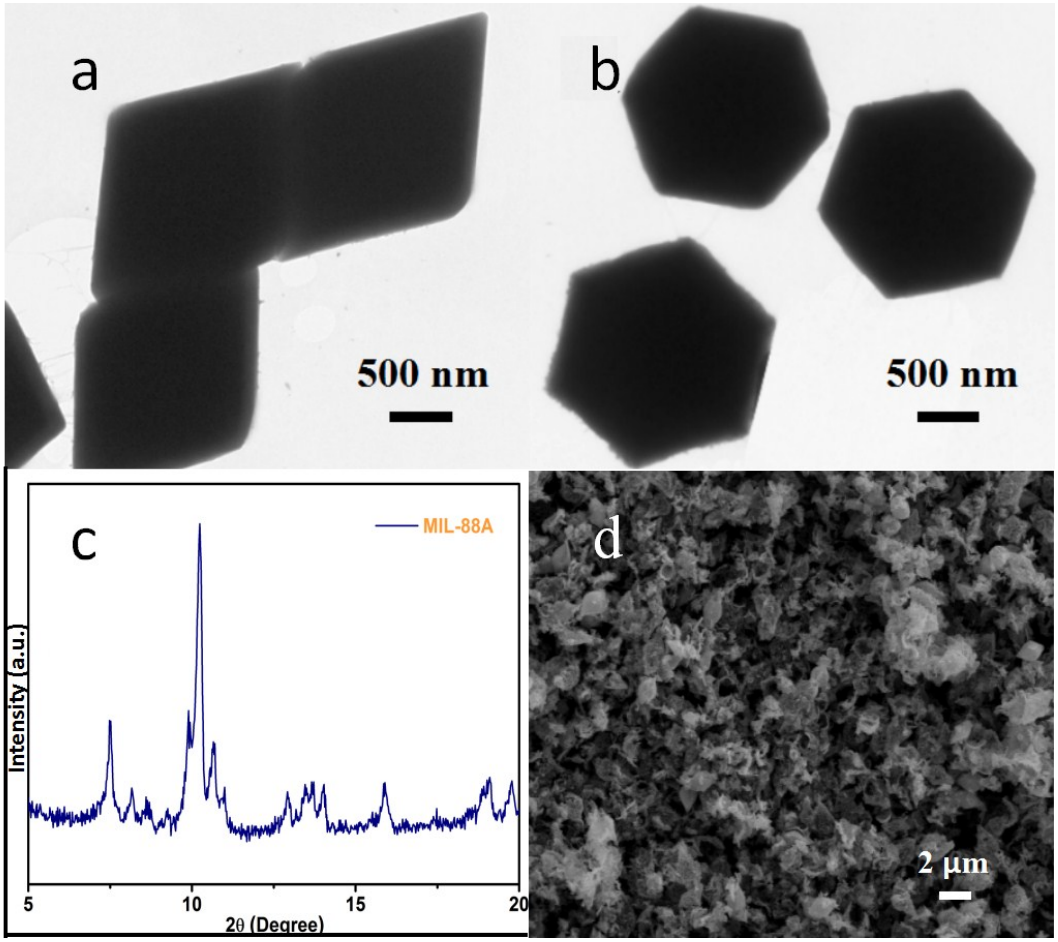

Fig. S1 (a, b) TEM and (c) XRD of the as-synthesized MIL-88A; (d) SEM image of MIL-88A heated at 500 ^{o}C for 4h.

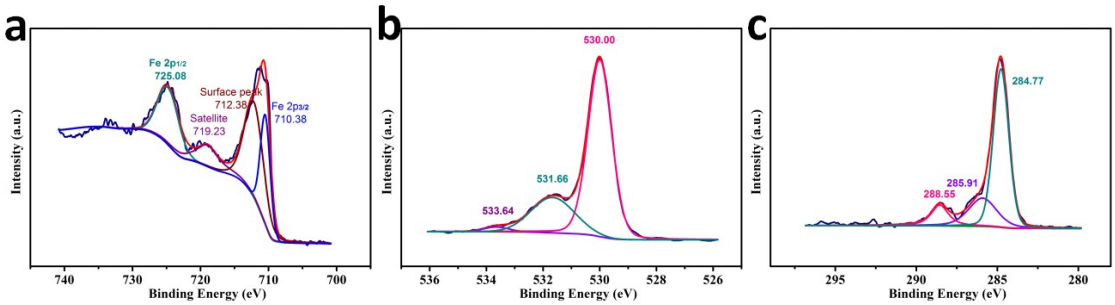

Fig. S2 XPS spectra of carbon-coated α-Fe_2O_3 hollow nanospindles.

As displayed in Fig. S2a, it reveals the peaks of Fe 2p at 710.38 eV and 725.08 eV , which match well with the reported values of Fe_2O_3. The deconvolution peaks of the O 1s spectrum (Fig. S2b) are decomposed into three components using peak fitting, which are centered at 530.00, 531.66 and 533.64 eV. One peak centered at 530.00 eV is attributed to the O^{2-} forming oxides with Fe, while the others can be ascribed to the -OH and -COOH in carbon, respectively. From the typical C 1s spectrum (Fig. S2c) in the composites, three components are also seen at 284.77, 285.91 and 288.55 eV, which correspond to the C-C, C-O and C=O bonds of carbon, respectively.

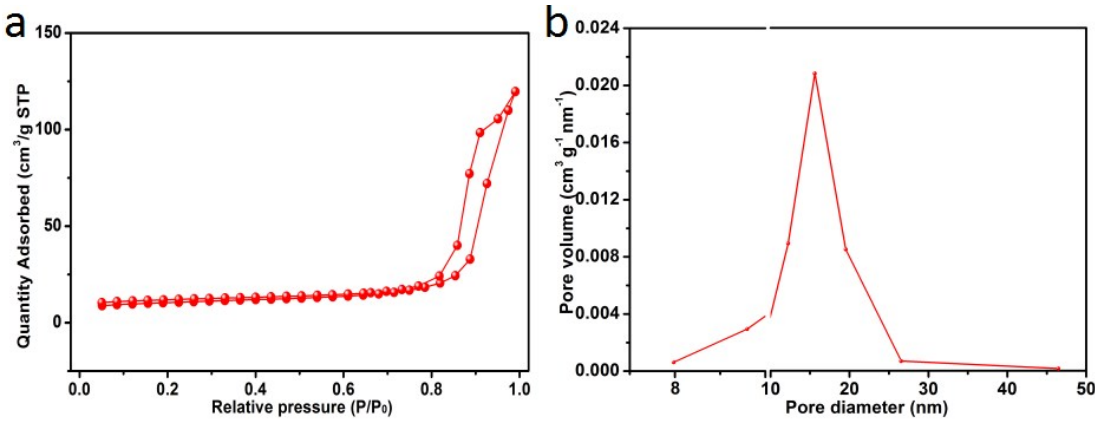

Fig. S3 (a) N_2 sorption isotherms and (b) pore size distributions of carbon-coated α-Fe_2O_3 hollow nanospindles.

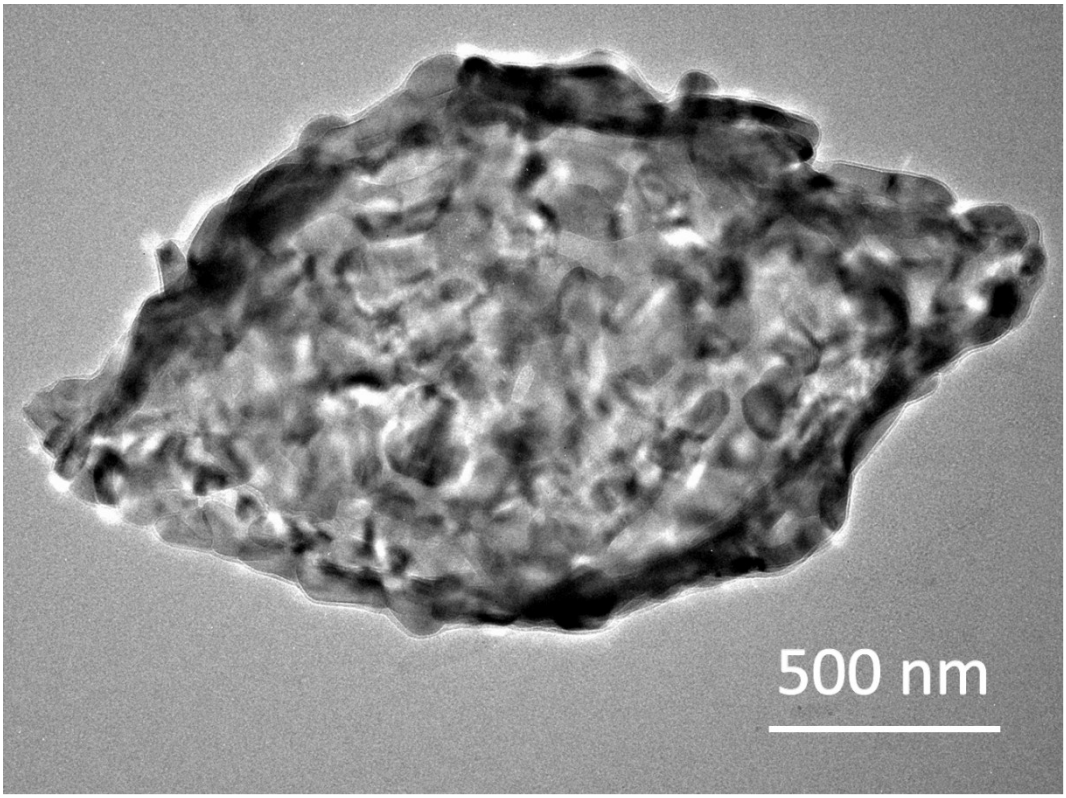

Fig. S4 Enlarged TEM image of carbon-coated α-Fe_2O_3 hollow nanospindle.

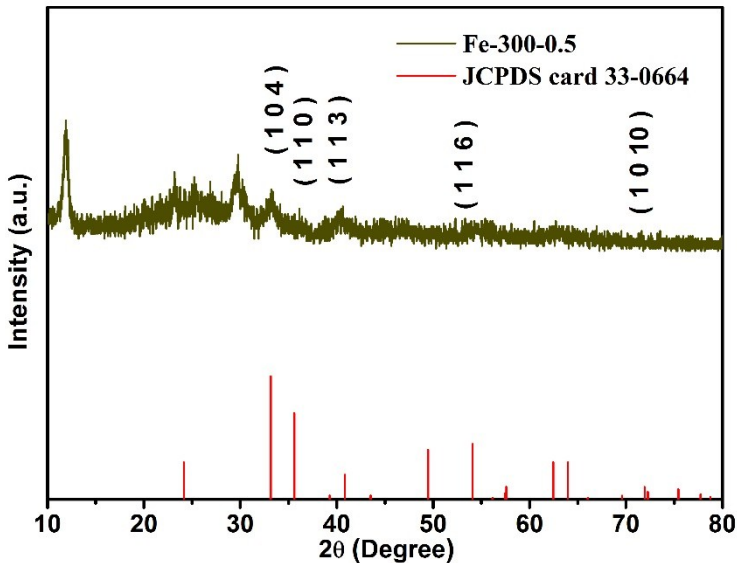

Fig. S5 XRD of Fe_2O_3-300-0.5.

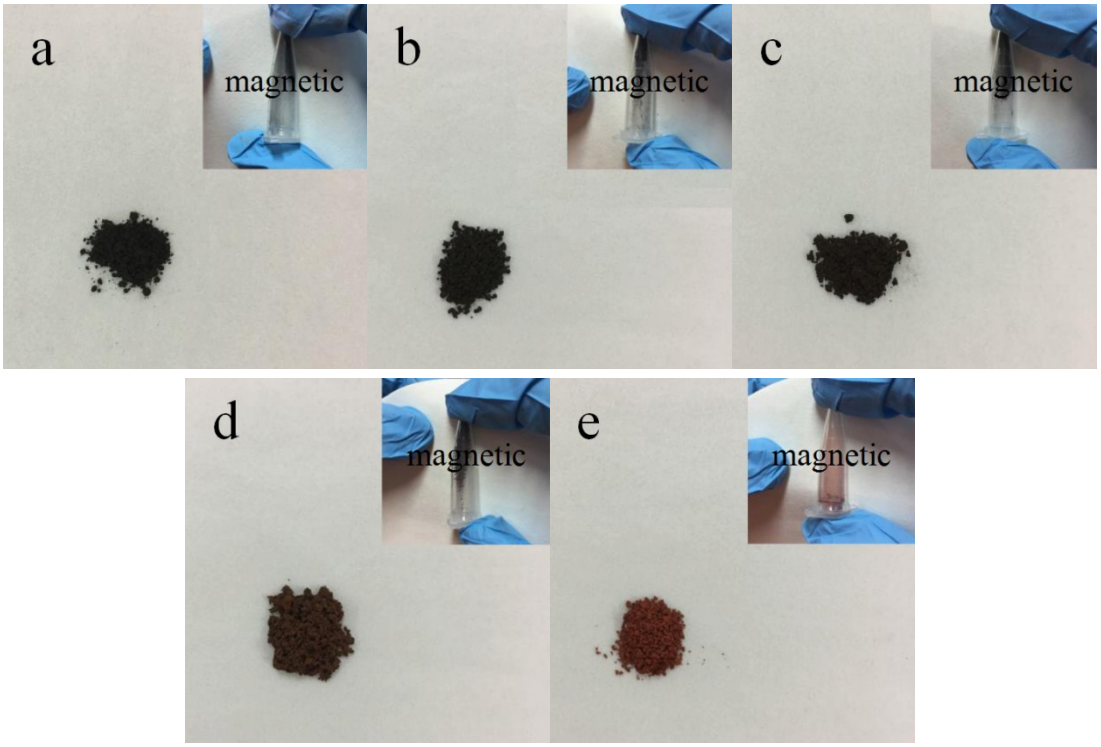

Fig. S6 Photographs of (a) Fe_2O_3-400-0.5, (b) Fe_2O_3-400-1, (c) Fe_2O_3-400-2, (d) Fe_2O_3-400-3 and (e) Fe_2O_3-500-2 spreaded on papers and magnetically suspended.

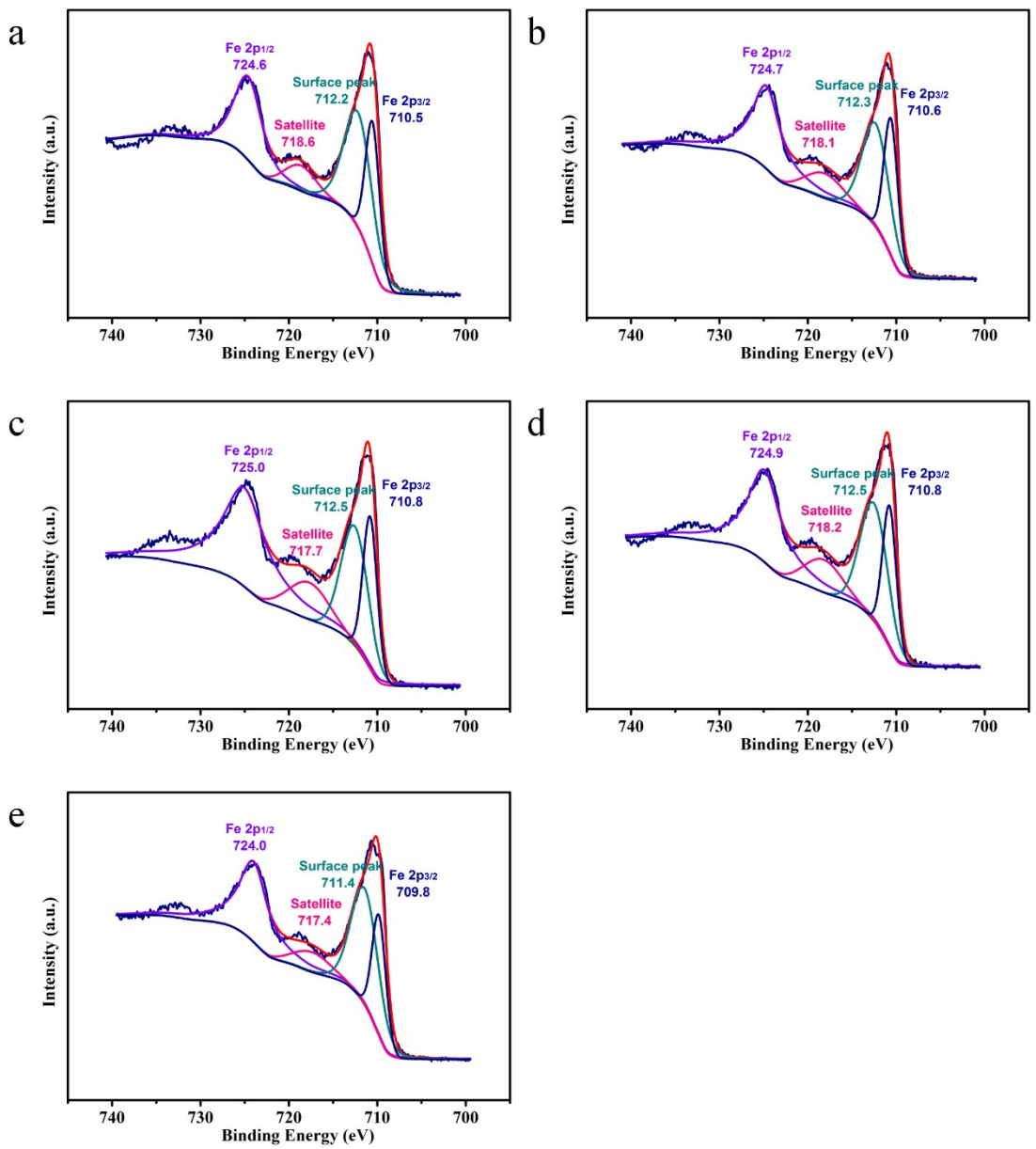

Fig. S7 XPS spectra (Fe 2p) of (a) Fe_2O_3-400-0.5, (b) Fe_2O_3-400-1, (c) Fe_2O_3-400-2, (d) Fe_2O_3-400-3 and (e) Fe_2O_3-500-2.

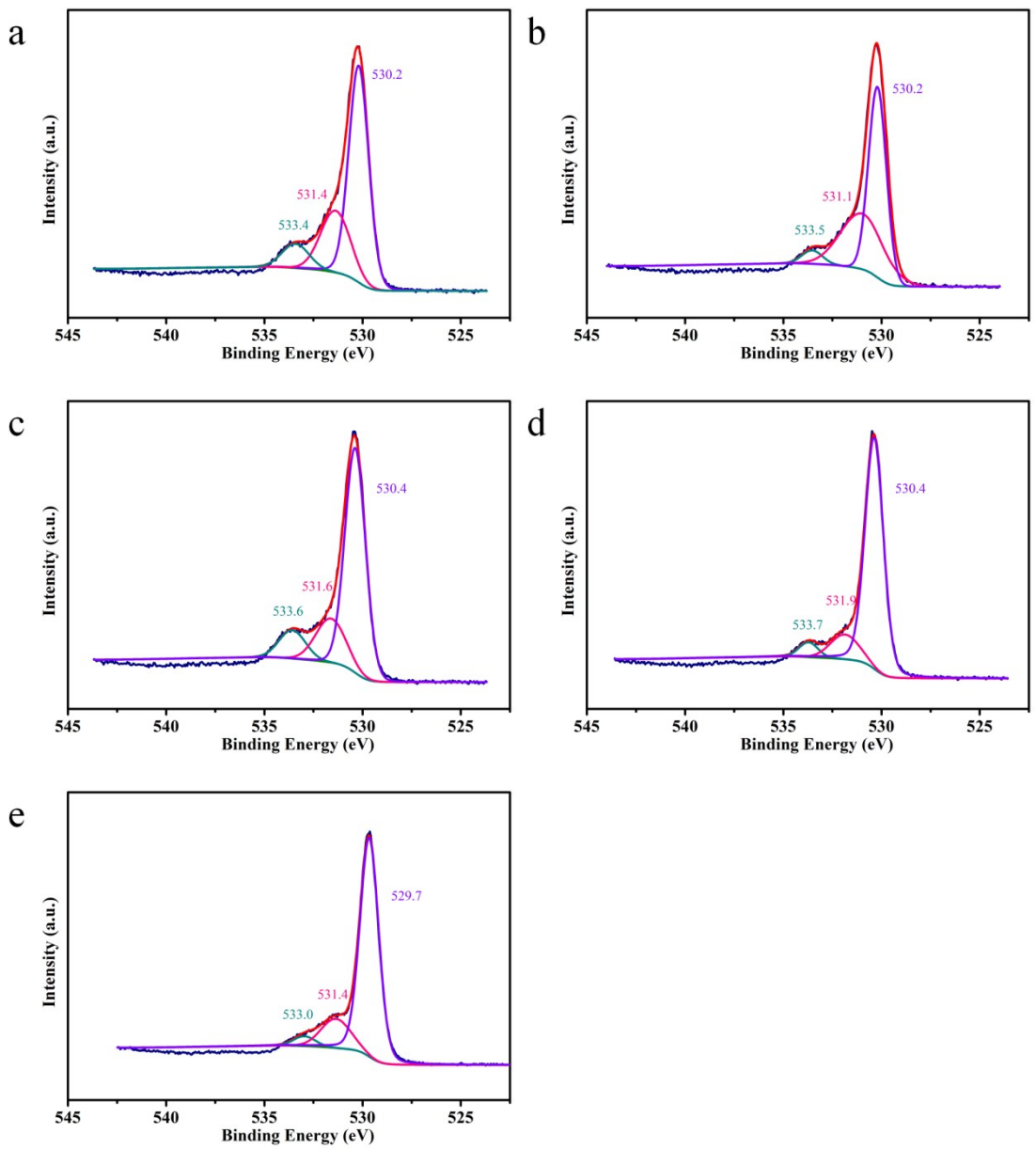

Fig. S8 XPS spectra (O 1s) of (a) Fe_2O_3-400-0.5, (b) Fe_2O_3-400-1, (c) Fe_2O_3-400-2, (d) Fe_2O_3-400-3 and (e) Fe_2O_3-500-2.

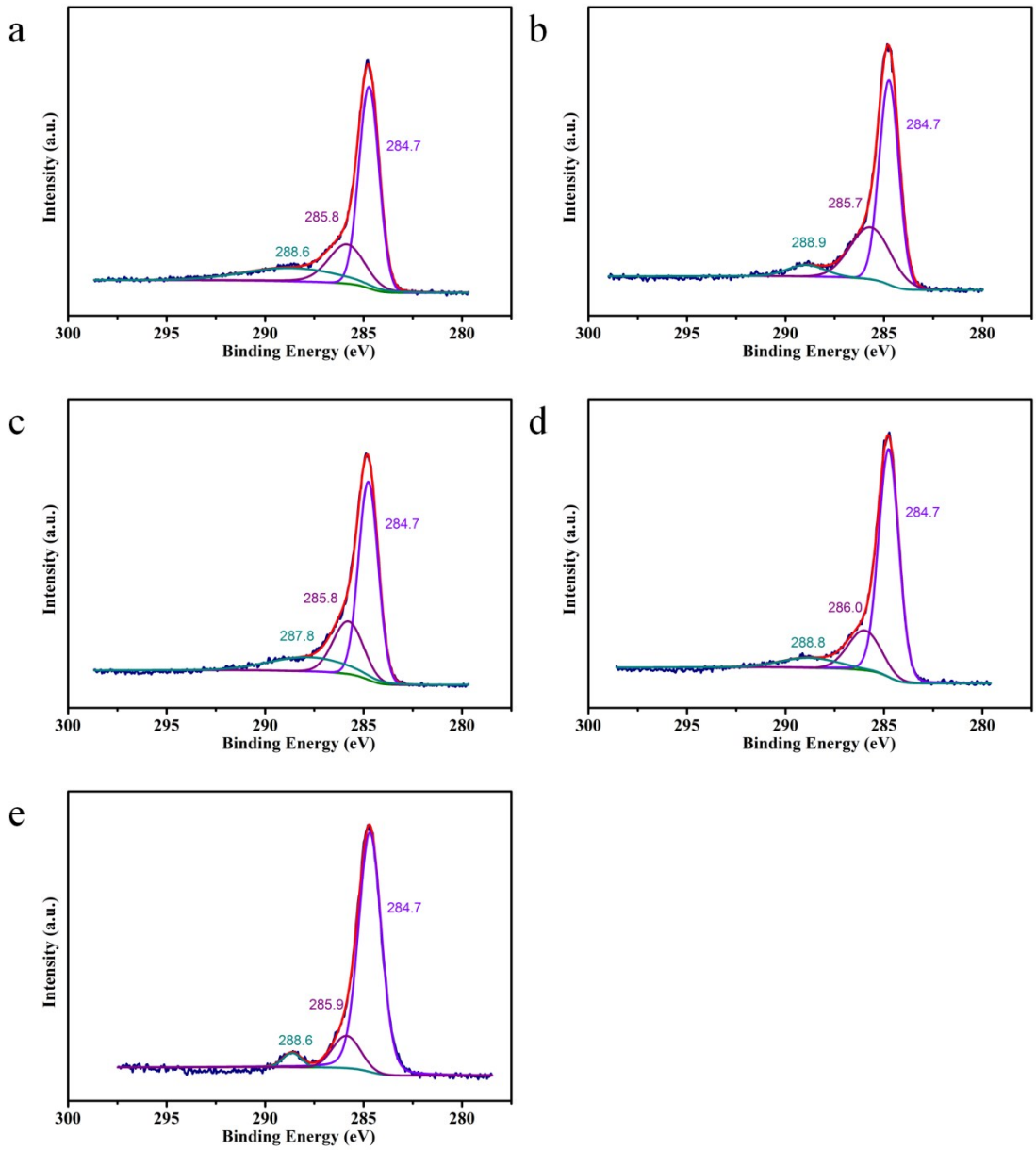

Fig. S9 XPS spectra (C 1s) of (a) Fe_2O_3-400-0.5, (b) Fe_2O_3-400-1, (c) Fe_2O_3-400-2, (d) Fe_2O_3-400-3 and (e) Fe_2O_3-500-2.

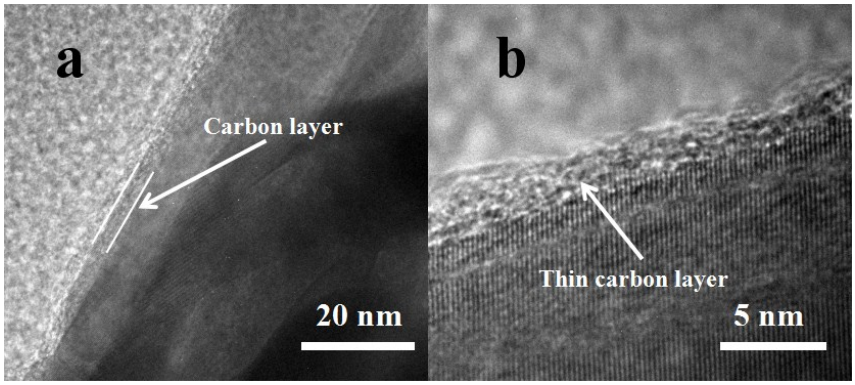

Fig. S10 HRTEM of Fe_2O_3-500-2.

The very little carbon on the surface of Fe_2O_3-500-2 nanobipyramids was found by TEM, which is similar to the preparation of MoO_2@C nano-octahedrons.[1]

(1) G. L. Xia, D. Liu, F. C. Zheng, Y. Yang, J. W. Su and Q. W. Chen, *J. Mater. Chem. A*, 2016, **4**, 12434-12441.

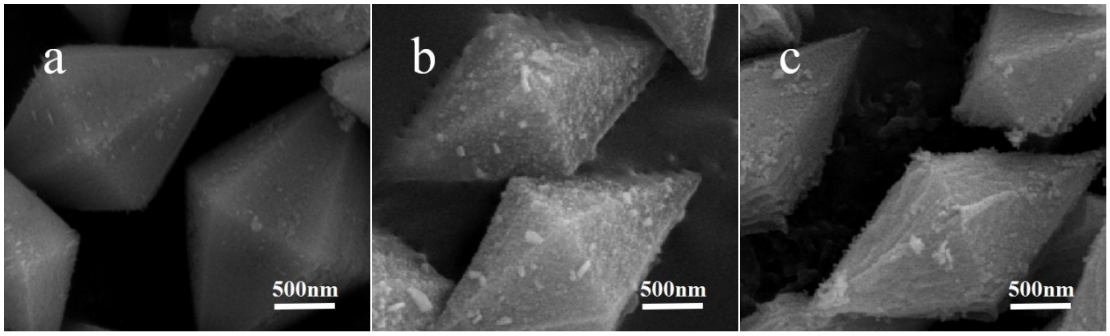

Fig. S11 SEM images of Fe_2O_3-300-0.5, Fe_2O_3-400-1, Fe_2O_3-400-3.

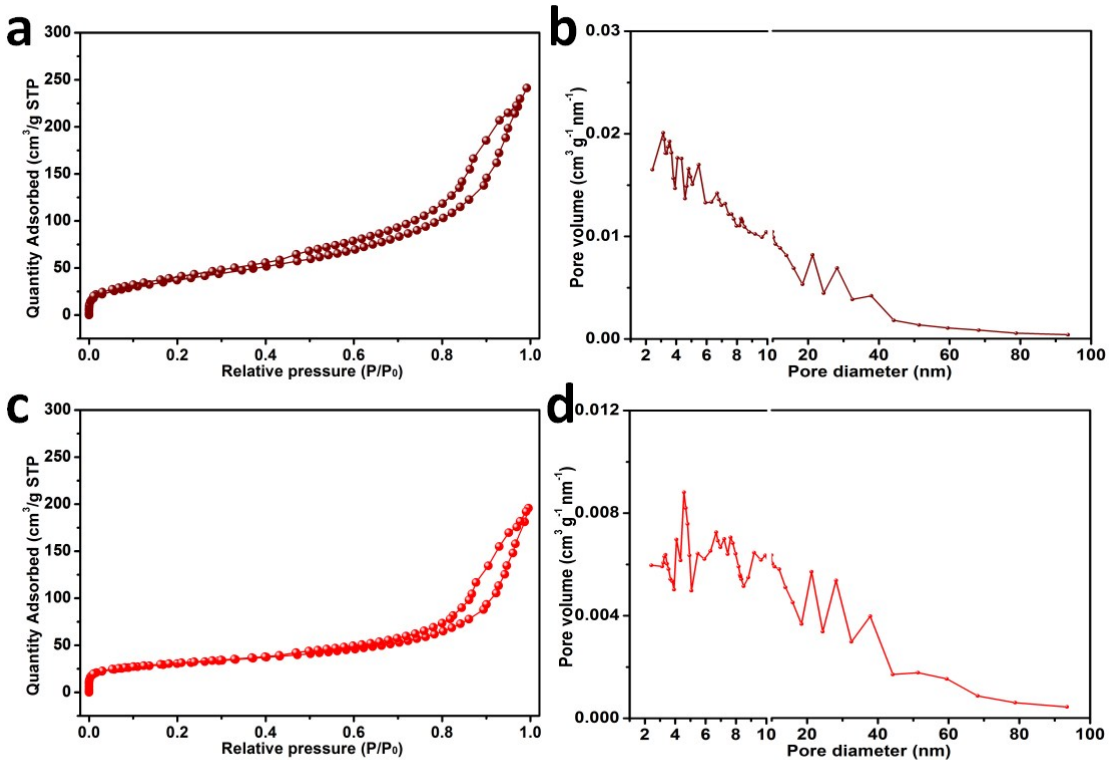

Fig. S12 (a) N_2 sorption isotherms and (b) pore size distributions of Fe-400-2; (c) N_2 sorption isotherms and (d) pore size distributions of Fe-500-2.

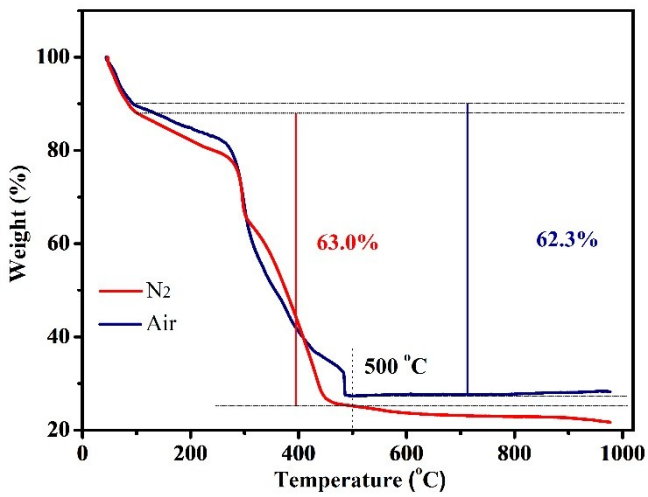

Fig. 13 (a) TGA curves of the MIL-88A precursors in air and N_2.

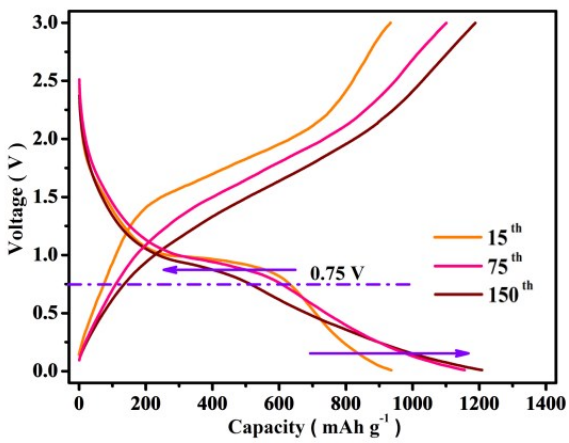

Fig. S14 The charge-discharge curves of α-Fe_2O_3 carbon-coating nanospheres for the 15th, 75th and 150th cycles at 0.2 C.

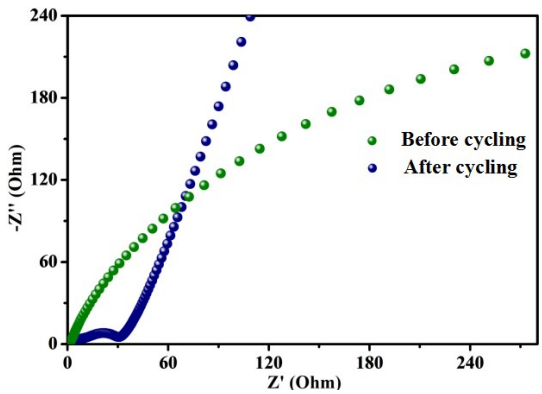

Fig. S15 EIS spectra of the carbon-coated α-Fe_2O_3 hollow nanospindles as anodes for LIBs before cycling and after cycling.

Table S1 Electrochemical properties of carbon-coated α-Fe_2O_3 hollow nanospindles, αγ-Fe_2O_3@C (Fe_2O_3-400-2) and α-Fe_2O_3@C nanobipyramids (Fe_2O_3-500-2) of this work and previous Fe_2O_3 derived from MOFs.

Typical examples	**Electrochemical properties**	**Ref.**
Carbon-coated α-Fe_2O_3 hollow nanospindles	1207 mAh g^{-1} after 200 cycles at a current density of 200 mAh g^{-1} 961.5 mAh g^{-1} after 500 cycles at a current density of 1000 mAh g^{-1}	**This work**
αγ-Fe_2O_3@C nanobipyramids	875.5 mAh g^{-1} after 50 cycles at a current density of 200 mAh g^{-1} 631.6 mAh g^{-1}after 150 cycles at a current density of 1000 mAh g^{-1}	**This work**
α-Fe_2O_3@C nanobipyramids	969.1 mAh g^{-1} after 50 cycles at a current density of 200 mAh g^{-1} 367.8 mAh g^{-1}after 150 cycles at a current density of 1000 mAh g^{-1}	**This work**
Porous Fe_2O_3 nanotubes	951.6 mAh g^{-1} after 50 cycles at a current density of 100 mA g^{-1}	[1]
α-Fe_2O_3 nano-assembled spindles	1024 mAh g^{-1} after 40 cycles at a current density of 100 mA g^{-1}	[2]
Spindle-like α-Fe_2O_3	911 mAh g^{-1}after 50 cycles at a current density of 200 mA g^{-1}	[3]
Porous Fe_2O_3 nanocubes	800 mAh g^{-1} after 50 cycles at a current density of 200 mA g^{-1}	[4]
Hierarchical Fe_2O_3 microboxes	945 mAh g^{-1} after 30 cycles at a current density of 200 mA g^{-1}	[5]
Multiple-shelled Fe_2O_3 microboxes	650 mAh g^{-1} after 30 cycles at a current density of 200 mA g^{-1}	[6]
Yolk−Shell octahedron	1176 mAh g^{-1} after 200 cycles at a current density of 100 mAh g^{-1} 744 mAh g^{-1}after 500 cycles at a current density of 1000 mAh g^{-1}	[7]

Table S2 Electrochemical properties of carbon-coated α-Fe_2O_3 hollow nanospindles, αγ-Fe_2O_3@C (Fe_2O_3-400-2) and α-Fe_2O_3@C nanobipyramids (Fe_2O_3-500-2) of this work and previous Fe_2O_3 or Fe_2O_3@C.

Typical examples	**Electrochemical properties**	**Ref.**
Carbon-coated α-Fe_2O_3 hollow nanospindles	1207 mAh g^{-1} after 200 cycles at a current density of 200 mAh g^{-1} 961.5 mAh g^{-1} after 500 cycles at a current density of 1000 mAh g^{-1}	**This work**
αγ-Fe_2O_3@C nanobipyramids	875.5 mAh g^{-1} after 50 cycles at a current density of 200 mAh g^{-1} 631.6 mAh g^{-1}after 150 cycles at a current density of 1000 mAh g^{-1}	**This work**
α-Fe_2O_3@C nanobipyramids	969.1 mAh g^{-1} after 50 cycles at a current density of 200 mAh g^{-1} 367.8 mAh g^{-1}after 150 cycles at a current density of 1000 mAh g^{-1}	**This work**
Porous α-Fe_2O_3 nanofibers	1180 mAh g^{-1}after 20 cycles at a current density of 100 mA g^{-1}	[8]
Mesoporous Fe_2O_3	800 mAh g^{-1}after 300 cycles at a current density of 500 mA g^{-1}	[9]
Polycrystalline α-Fe_2O_3 nanotubes	1000 mAh g^{-1} after 50 cycles at 0.5 C, 500-800 mAh g^{-1} at 1-2 C	[10]
Porous α-Fe_2O_3nanosheets on Ti foil	908 mAh g^{-1} after 60 cycles at a current density of 100 mA g^{-1}	[11]
Single crystalline α-Fe_2O_3 nanoshee- ts grown directly on Ni foam	518 mAhg $^{-1}$ after 50 cycles at 0.1 C	[12]
γ-Fe_2O_3/graphenenanoribbons	910 mAh g^{-1} after 134 cycles at acurrent density of 200 mA g^{-1}	[13]
Carbon-coated α-Fe_2O_3 hollow nan- ohorns grafted on CNTbackbones	800 mAh g^{-1} after 100 cycles at a current density of 500 mA g^{-1}	[14]
α-Fe_2O_3@rGO,core/shell composite	1787.27mAh g^{-1} after 90 cycles at acurrent density of 100 mA g^{-1}	[15]
3D porous α-Fe_2O_3 nanorods/CNT	1000 mAh g^{-1} after 300 cycles at acurrent density of 200 mA g^{-1}	[16]

-GFcomposite (GF: graphene foam)		
RG-O/Fe_2O_3 composite	1027 mAh g^{-1} after 50 cycles at acurrent density of 100 mA g^{-1}	[17]
Fe_2O_3/GS Aerogels	733 mAh g^{-1} after 1000 cycles at acurrent density of 2000 mA g^{-1}	[18]
40 wt.%-rGO/Fe_2O_3 composite	690 mAh g^{-1} after 100 cycles at acurrent density of 500 mA g^{-1}	[19]
Fe_2O_3-graphene sheet-on-sheet composites	800.6 mAh g^{-1} after 50 cycles at acurrent density of 100 mA g^{-1}	[20]
Fe_2O_3/Fe_3C-graphene thin film	518 mAh g^{-1} after 100 cycles at acurrent density of 0.17 C	[21]
Fe_2O_3@C@G composite	864 mAh g^{-1} after 100 cycles at acurrent density of 100 mA g^{-1}	[22]
Fe_2O_3-FLG composite	758 mAh g^{-1} after 300 cycles at acurrent density of 200 mA g^{-1}	[23]
Fe_2O_3/rGO composite	600 mAh g^{-1} at acurrent density of 200 mA g^{-1}	[24]
HP-Fe-G composite	1100 mAh g^{-1} after 50 cycles at acurrent density of 50 mA g^{-1}	[25]
Fe_2O_3-NC/GN aerogels	1121 mAh g^{-1} after 500 cycles at acurrent density of 500 mA g^{-1}	[26]
rGO/α-Fe_2O_3 nanoplate composite	896 mAh g^{-1} after 200 cycles at acurrent density of 5 C	[27]
Fe_2O_3-GNS rice (or particle)-on-sheet composite	734 mAh g^{-1} after 40 cycles at acurrent density of 0.1 C	[28]
α-Fe_2O_3/CNT-GF composite	1000 mAh g^{-1} after 300 cycles at acurrent density of 200 mA g^{-1}	[29]
α-Fe_2O_3 nanorod arrays on reduced graphene oxide	1200 mAh g^{-1} after 500 cycles at acurrent density of 200 mA g^{-1}	[30]

References:

(1) M. C. Sun, M. F. Sun, H. X. Yang, W. H. Song, Y. Nie and S. N. Sun, *Ceram. Int.*, 2017, **43**, 363-367.

(2) A. Banerjee, V. Aravindan, S. Bhatnagar, D. Mhamane and S. Madhavi, Ogale. S. *Nano Energy*, 2013, **2**, 890-896.

(3) X. D. Xu, R. G. Cao, S. Jeong and J. Cho, *Nano Lett*., 2012, **12**, 4988-4991.

(4) L. Zhang, H. B. Wu, R.Xu and X. W. Lou, *CrystEngComm*, 2013, **15**, 9332-9335.

(5) L. Zhang, H. B.Wu, S. Madhavi, H. H. Hng and X. W. Lou, *J. Am. Chem. Soc.*, 2012, **134**, 17388-17391.

(6) L. Zhang, H. B. Wu and X. W. Lou, *J. Am. Chem. Soc.*, 2013, **135**, 10664-10672.

(7) W. Guo, W. Sun, L. P. Lv, S.Kong and Y. Wang, *ACS Nano*, 2017, **11**, 4198-4205.

(8) S. Jayaraman, V. Aravindan, M. Ulaganathan, W. C. Ling, S. Ramakrishna and S. Madhavi, *Adv. Sci*., 2015, 1500050.

(9) Y. Xu, G. Jian, Y. Liu, Y. Zhu, M. R. Zachariah and C. Wang, *Nano Energy*, 2014, **3**, 26-35.

(10) Z. Y. Wang, D. Y. Luan, S. Madhavi, C. M. Li and X. W. Lou, *Chem. Commun.*, 2011, **47**, 8061-8063.

(11) L. L. Li, H. B. Wu, L. Yu, S. Madhavi and X. W. Lou, *Adv. Mater. Interfaces,* 2014, **1**, 1400050.

(12) D. N. Lei, M. Zhang, B. H. Qu, L. B.Chen, Y. G.Wang, E. D. Zhang, Z. Xu, Q. H. Li and T. H. Wang, *Nanoscale*, 2012, **4**, 3422-3426.

(13) J. Lin, A. R. O. Raji, K. Nan, Z. Peng, Z. Yan, E. L.Samuel, D. Natelson and J. M. Tour, *Adv. Funct. Mater.*, 2014, **24**, 2044-2048.

(14) Z. Y. Wang, D. Y. Luan , S. Madhavi, Y. Hu and X. W. Lou, *Energy Environ. Sci.*, 2012, **5**, 5252-5256.

(15) X. Li, Y. Ma , L. Qin, Z. Zhang, Z. Zhang, Y. Z. Zheng and Y. Qu, *J. Mater. Chem. A*, 2015, **3**, 2158-2165.

(16) M. Chen, J. Liu, D. Chao, J. Wang, J. Yin, J. Lin, H. J. Fanand and Z. X. Shen, *Nano Energy*, 2014, **9**, 364-372.

(17) X. Zhu, Y. Zhu, S. Murali, M. D. Stoller and R. S. Ruoff, *ACS Nano*, 2011, **5**, 3333-3338.

(18) R. H. Wang, C. H. Xu, M. Du, J. Sun, L. Gao, P. Zhang, H. L. Yao and C. C. Lin, *Small*, 2014, **10**, 2260-2269.

(19) I. T. Kim, A. Magasinski, K. Jacob and G. Yushin, *Carbon*, 2013, **52**, 56-64.

(20) J. Kan and Y. Wang, *Sci. Rep.*, 2013, **3**, 3502.

(21) Y. Yang, X. J. Fan, G. Casillas, Z. W. Peng, G. D. Ruan, G. Wang, M. J. Yacaman and J. M.Tour, *ACS Nano*, 2014, **8**, 3939-3946.

(22) H. L. Fei, Z. W. Peng, L. Li, Y. Yang, W. Lu, E. L. G. Samuel, X. J. Fan and J. M. Tour, *Nano Res.*, 2014, **7**, 502-510.

(23) Y. K. Wang, L. C. Yang, R. Z. Hu, W. Sun, J. W. Liu, L. Z. Ouyang, B. Yuan, H. H. Wang and M. Zhu, *J. Power Sources*, 2015, **288**, 314-319.

(24) L. S. Xiao, M. Schroeder, S. Kluge, A. Balducci, U. Hagemann, C. Schulz and H. Wiggers, *J. Mater. Chem. A*, 2015, **3**, 11566-11574.

(25) X. Wang, W. Tian, D. Q. Liu, C. Y. Zhi, Y. Bando and D. Golberg, *Nano Energy*, 2013, **2**, 257-267.

(26) R. H. Wang, C. H. Xu, J. Sun and L. Gao, *Sci. Rep.*, 2014, **4**, 7171.

(27) S. K. Liu, Z. X. Chen, K. Xie, Y. J. Li, J. Xu and C. M. Zheng, *J. Mater. Chem. A*, 2014, **2**, 13942-13948.

(28) Y. Q. Zou, J. Kan and Y. Wang, *J Phys. Chem. C*, 2011, **115**, 20747-20753.

(29) M. H. Chen, J. L. Liu, D. L. Chao, J. Wang, J. H. Yin, J. Y. Lin, H. J. Fan and Z. X. Shen, *Nano Energy*, 2014, **9**, 364-372.

(30) D. Z. Kong, C. W. Cheng, Y. Wang, B. Liu, Z. X. Huang and H. Y. Yang, *J. Mater.Chem. A*, 2016, **4**, 11800-11811.